Some aspects of interlaminar toughening: reactively terminated thermoplastic particles in thermoset composites*

P. T. McGrail and S. D. Jenkins†
ICI Materials, Wilton Materials Research Centre, Wilton, Middlesbrough, Cleveland TS6 8JE, UK
(Received 30 April 1992; revised 30 June 1992)

Novel, reactively terminated, polysulphone thermoplastics have been used as particulate interlaminar toughening agents in epoxy, bismaleimide, and cyanate ester resin based composites. These particles dissolved completely into each thermoset resin matrix during cure, resulting in two separate toughening mechanisms. A crack front pinning type toughening was observed at low particle areal densities in the interlaminar regions ($<3\times10^3$ particles cm^{-2}), whilst a toughened film interleaf effect was produced at high particle areal densities ($>6\times10^3$ particles cm^{-2}). The fracture toughness, G_{1c}, of one epoxy composite was improved from $0.51\pm0.07\,kJ\,m^{-2}$ to $0.77\pm0.10\,kJ\,m^{-2}$, with no drop in interlaminar shear strength. Compression after impact testing of the cyanate ester composite at $6.67\times10^3\,J\,m^{-1}$ revealed a decrease in delamination area from $28.2\pm3.0\,cm^2$ to $11.6\pm1.5\,cm^2$ with interlaminar toughening. Compression resistance rose accordingly from 223.4 ± 0.7 MPa to 268.9 ± 15.9 MPa. This was achieved for a laminate weight increase of only 1.1%.

(Keywords: polysulphone; interlaminar toughening; thermoset composite; impact)

INTRODUCTION

Interlaminar toughening (ILT) has recently been recognized as a simple means of improving the impact resistance of thermoset resin matrix, continuous fibre composites[1–6]. The technique involves incorporating usually heterogeneous organic or inorganic particles[1,2], flock[3], short fibres[4], or films[5,6], in the interlaminar regions of the composite (i.e. between the prepreg plies). Technology for achieving this, therefore, varies from simple spray coating of the prepreg[1,2], to quite complex filming processes[6]. Impact resistance is an important quality for such composites, particularly in aerospace applications. Many manufacturers in this field routinely adopt a low energy impact test [for example compression after impact (CAI)][7] to quantify resulting delamination. As pressure increases to further utilize the weight-saving advantages of these materials, their use in primary aircraft structure will become more common. Hence interest in ILT to combat delamination on impact is also likely to grow.

In this work, various novel, reactively terminated, polysulphone thermoplastics were used as particulate ILT agents in epoxy, bismaleimide, and cyanate ester resin based composites. Laminate fracture toughness, G_{1c}, interlaminar shear strength (ILSS) and CAI properties[7,8] were studied, as a function of ILT particle areal density on the prepreg. The effect on these parameters of changing the end group functionality of the polysulphone thermoplastic used (from reactive to non-reactive with respect to the crosslinking chemistry), was also examined for the bismaleimide composite.

EXPERIMENTAL

A range of toughened epoxy/carbon fibre prepregs was used as supplied by ICI Fiberite (Hy-E 1374BM, Hy-E 1377-1T, Hy-E 1377-2T and Hy-E 1377-3T), in the form of unidirectional tapes. The Hy-E 1377 materials differ from Hy-E 1374BM in that they adopt a co-continuous morphology on curing as the blended thermoplastic toughening agent phase separates[9–11]. The bismaleimide and cyanate ester/carbon fibre prepregs were also blend-toughened unidirectional tapes (Hy-E 1686N and Hy-E 1354-2T, respectively), the latter having a co-continuous morphology. All of these materials had ~35% w/w resin content, at $145\,g\,m^{-2}$ fibre areal weight. The polysulphone thermoplastics used are proprietary to ICI, and consequently details of their chemical structure cannot be given. For the purposes of this work they will be called: thermoplastic A (reactively terminated); thermoplastic B (non-reactively terminated, otherwise identical to A); and thermoplastic C (reactively terminated at slightly higher molecular weight, otherwise identical to A). Thermoplastic powders A and C had a mean particle diameter of ~80 μm while for thermoplastic powder B this was ~40 μm. Their particle size distributions were as shown in *Figures 1a* and *b*.

The examples of ILT listed in *Table 1* were considered. For combinations 1–3, the thermoplastic particles were sieved onto the prepreg to give uniform coatings at 0, 0.5, 1, 1.5, 2, 2.5, 3, 6, 9 and 12% w/w of the uncured prepreg. These loadings corresponded to ILT particle

* Presented at 'Advances in Polymeric Matrix Composites', 5–10 April 1992, San Francisco, CA, USA
† To whom correspondence should be addressed

0032-3861/93/040677-07

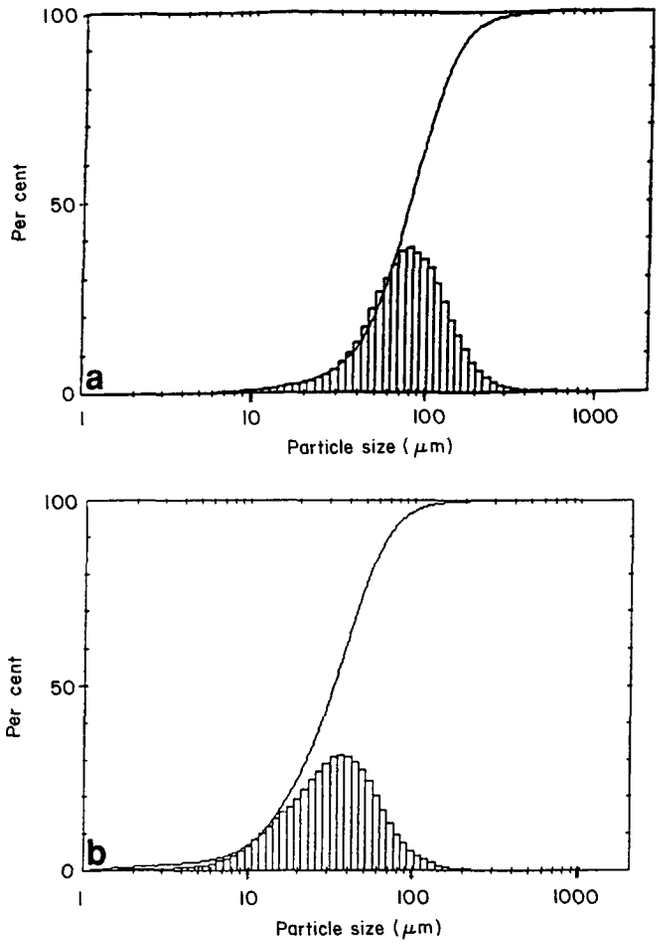

Figure 1 Typical ILT particle size distributions for (a) thermoplastic powders A and C, and (b) thermoplastic powder B

Table 1 ILT combinations and mechanical tests used in this work

Combination	Matrix resin	Prepreg	Thermoplastic	Test method
1	Epoxy	Hy-E 1374BM	A	DCB, ILSS
2	BMI[a]	Hy-E 1686N	A	DCB, ILSS
3	BMI[a]	Hy-E 1686N	B	DCB, ILSS
4	Epoxy	Hy-E 1377-1T	C	CAI
5	Epoxy	Hy-E 1377-2T	C	CAI
6	Epoxy	He-E 1377-3T	C	CAI
7	Cyanate	Hy-E 1354-2T	C	CAI

[a] BMI = Bismaleimide

areal densities on the prepreg of 0 to $\sim 12 \times 10^3$ particles cm^{-2}. For combinations 4–7, the thermoplastic particles were sprayed by air gun onto the prepreg: for combination 4, $\sim 3.4 \times 10^3$ particles cm^{-2} of thermoplastic C was used (3.4% w/w of the uncured prepreg); for combination 5, ~ 2.6 and 4.9×10^3 particles cm^{-2} (2.6 and 4.9% w/w); for combination 6, $\sim 3.1 \times 10^3$ particles cm^{-2} (3.1% w/w); and for combination 7, ~ 1.0, 1.1, 1.2 and 2.0×10^3 particles cm^{-2} (1.0–2.0% w/w). The levels of loading were less controllable with the air gun spraying technique, as they could only be monitored by weighing the sprayed laminate before cure. There was no accurate method for predetermining the loading (as in the sieved examples), due to the loss of particles during the spraying process. The sieved laminates were also weighed pre-cure to confirm their loadings.

Unidirectional laminates ($[0]_{24}$) measuring 12.5 cm(0) × 10 cm(90) were made at each loading for combinations 1–3. An aluminium foil crack starter was placed between the centre plies of each sample, to facilitate double cantilever beam (DCB) testing[8]. For combinations 4–7 the lay up was $[+45, 0, -45, 90]_{4s}$, with the laminates 35 cm(90) × 25 cm(0) in size. This allowed four samples of 15 cm(90) × 10 cm(0) to be cut for 6.67×10^3 J m^{-1} testing from each. The cure and post-cure cycles used for combinations 1–7 were as recommended by ICI Fiberite. In brief, combinations 1 and 4–6 were cured at 180°C for 2 h under 551.6 kPa nitrogen pressure, whilst combinations 2, 3, and 7 were also cured at 180°C but for 4 h under 620.6 kPa nitrogen pressure, and post-cured at 240°C for 6 h (2 and 3) or 2 h (7) freestanding. Testing for ILSS was performed on combinations 1–3 only. The hot/wet conditions for combinations 1 and 2 were: testing at 82°C (hot), after immersion in water for 7 days at 71°C (wet).

RESULTS AND DISCUSSION

Combinations 1–3

Figures 2–4 show electron micrographs of the interlaminar regions for combinations 1–3 respectively, (polished and etched sections perpendicular to the fibre direction, where the thermoplastic-rich phase has been preferentially etched). In *Figure 2* a particulate morphology has been produced at the dissolution site of a particle of thermoplastic A. Thermoplastic-rich nucleii have been etched from a localized epoxy-rich zone. Both phases in this morphology are thought to be mixtures of the epoxy resin and thermoplastic A. Such phase separation in thermoset/thermoplastic blends during cure has been well documented[9–11]. The background morphology in this sample (away from the interlaminar zone), is also formed by phase separation, but of the blended thermoplastic toughening agent in the matrix, not the ILT agent.

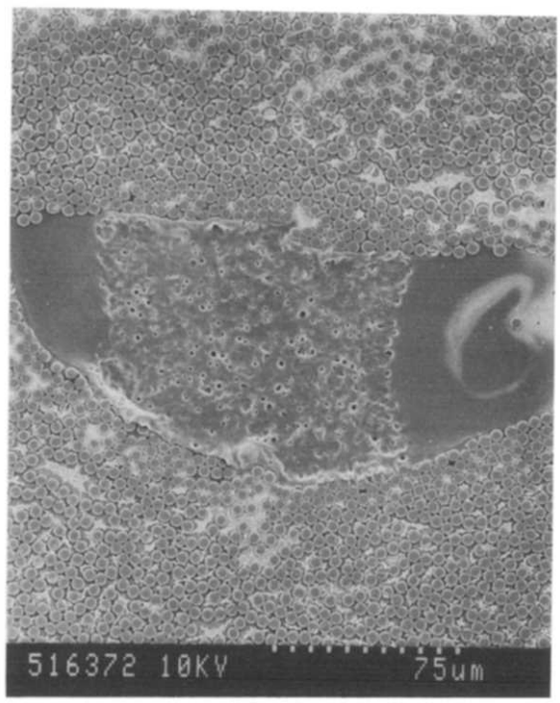

Figure 2 Particulate morphology at the dissolution site of a thermoplastic A particle in Hy-E 1374BM

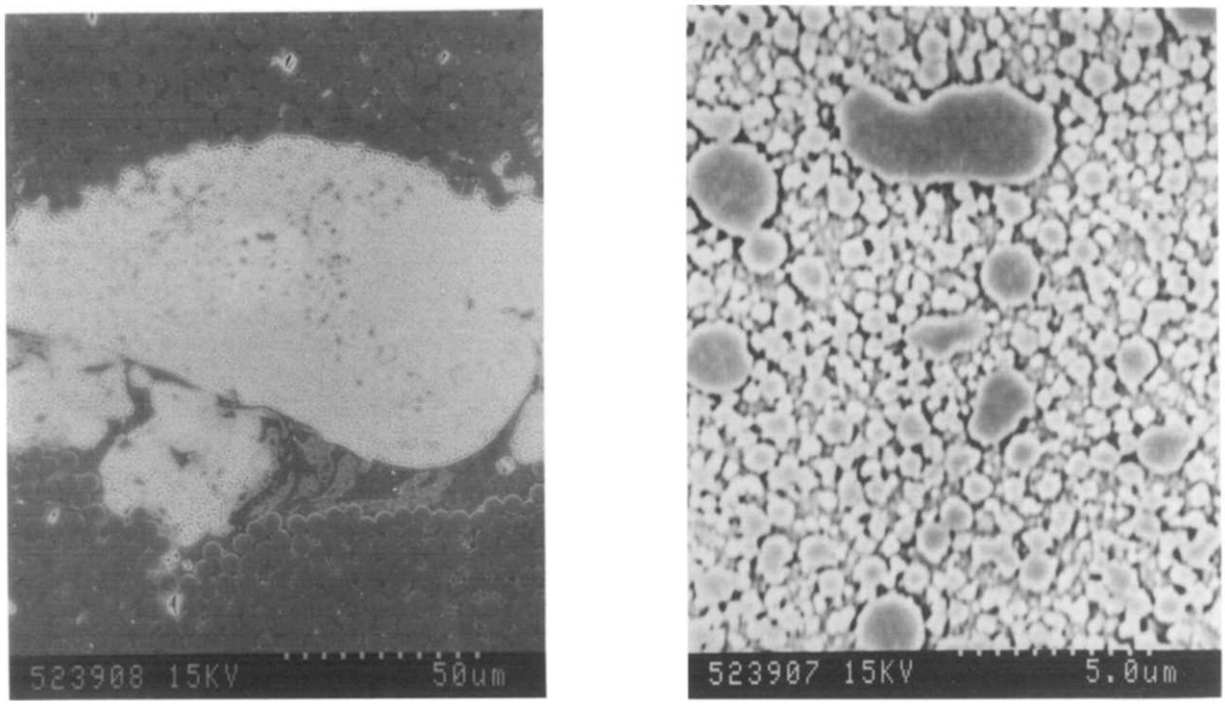

Figure 3 Phase-inverted morphology at the dissolution site of a thermoplastic A particle in Hy-E 1686N at two magnifications

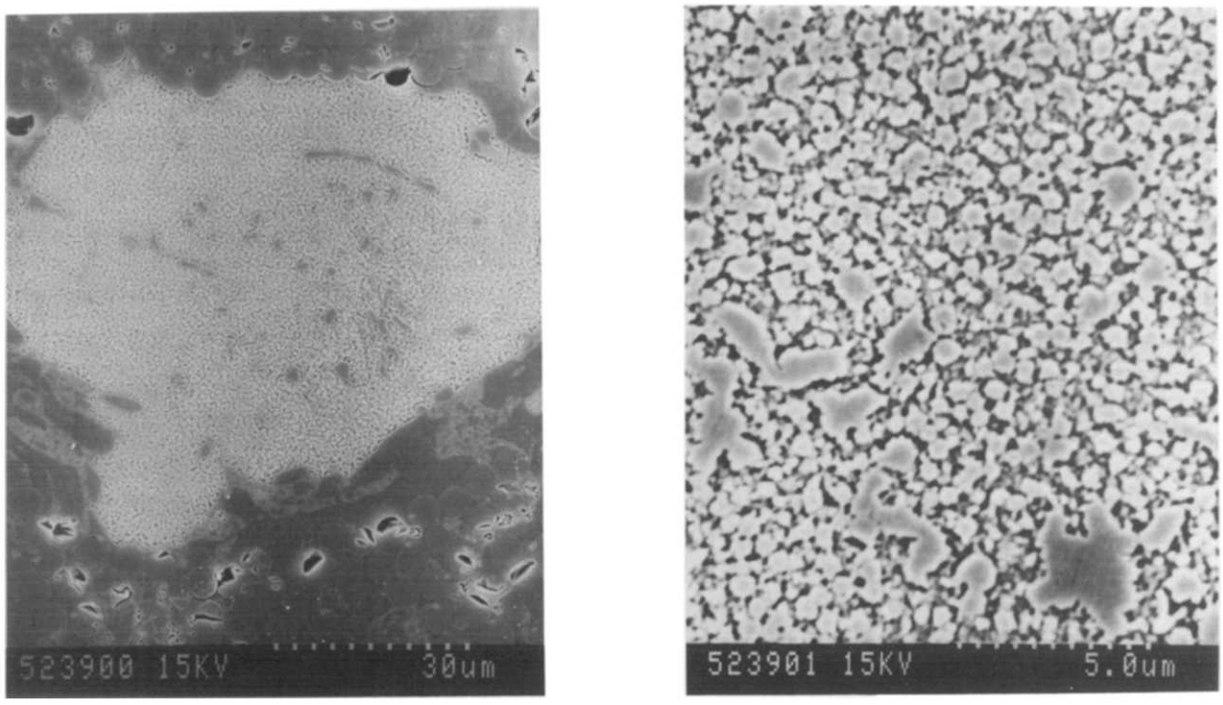

Figure 4 Phase-inverted morphology at the dissolution site of a thermoplastic B particle in Hy-E 1686N at two magnifications

Figures 3 and *4* show much the same situation for combinations 2 and 3. Here however, in both cases, a phase-inverted morphology has been formed at the dissolution sites of the respective ILT agents[9–11]. This has resulted in a localized thermoplastic-rich continuum (with thermoplastic A or B, respectively), containing bismaleimide-rich islands. Both phases in each of these morphologies are thought to be mixtures of thermoset and thermoplastic as above. The background morphologies again show evidence of phase separation of the blended thermoplastic toughening agent. The change in morphology with thermoplastic A in combinations 1 and 2 (particulate to phase-inverted), is not unexpected, as phase separation is strongly dependent on the chemical and physical properties of the thermoset and thermoplastic concerned[9,10]. A phase-inverted morphology at the dissolution sites suggests a greater incompatibility of the thermoplastic with the thermoset. Phase separation has possibly occurred earlier in the cure cycle for combination 2, and coarsening to give the phase-inverted morphology has had time to occur, prior to gelation. It is thus somewhat surprising that the

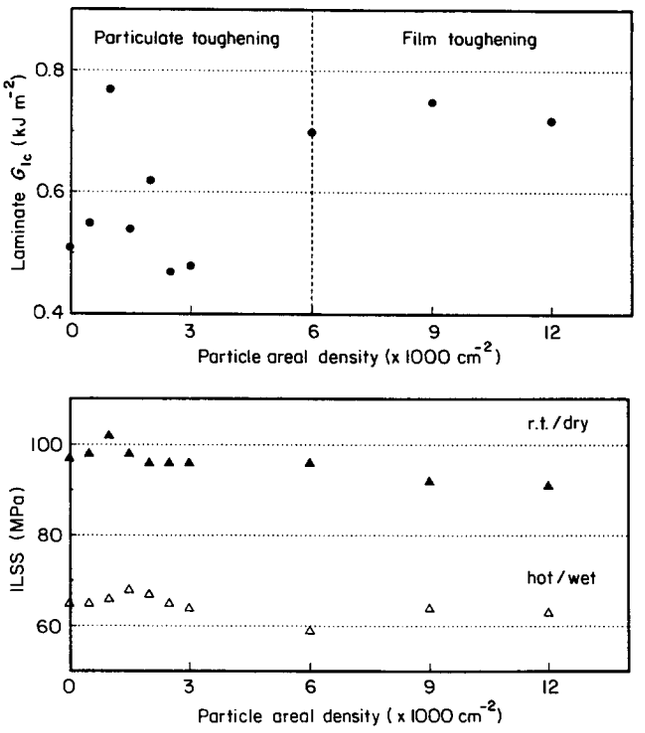

Figure 5 Laminate G_{1c} and ILSS for Hy-E 1374BM, with thermoplastic A as the ILT agent

morphologies in combinations 2 and 3 are so similar, even to scale size. It would appear, therefore, that the end group functionality of the thermoplastic ILT agent alone has little direct effect on phase separation.

Figures 5 and *6* show the effect on laminate G_{1c} and ILSS of the ILT particle areal density on the prepreg for combinations 1–3. For combinations 1 and 2, two separate toughening effects were identified. At $<3\times10^3$ particles cm^{-2} each had a maximum in laminate G_{1c} (~1.0 and 1.5×10^3 particles cm^{-2}, respectively). Values of 0.77 ± 0.10 kJ m^{-2} (an increase of 51% on the control value of 0.51 ± 0.07 kJ m^{-2}) in combination 1, and 0.70 ± 0.10 kJ m^{-2} (an increase of 63% on the control value of 0.43 ± 0.06 kJ m^{-2}) in combination 2, were recorded. At $>6\times10^3$ particles cm^{-2} a plateau of improved toughness was reached in each case. Here the average laminate G_{1c} values were 0.72 ± 0.10 kJ m^{-2} for combination 1 (a 41% increase on the control), and 0.71 ± 0.10 kJ m^{-2} for combination 2 (a 65% increase on the control). For combination 3, however, no improvement in toughness was observed (see *Figure 6*).

For the low ILT particle areal densities, toughening was thought to be the result of crack path deviation, crack front pinning, or some similar particulate toughening mechanism[8,12]. Provided the crack remains in the interlaminar region, the crack front pinning model could at least qualitatively describe the origin of the maximum in laminate G_{1c} observed. Consider the perimeter of each dissolution site to define a final particle diameter. Laminate G_{1c} is increased in this scenario as the crack front travels freely between such particles, but is pinned at them, as a result of which it is bowed. More energy is then required to continue crack propagation, due to the increased crack front area. As the ILT particle areal density increases, and dissolution sites encroach closer together, the crack front may then 'see' large agglomerated pinning points rather than individual sites. The number of active pinning points is thus decreased, hence reducing the toughening effect[12]. For crack front pinning to occur, therefore, the final particle diameter (as defined above) should be much less than the original interparticle spacing on the prepreg.

For the high ILT particle areal densities, the secondary improvement in laminate G_{1c} was thought to occur due to crack propagation through a toughened film, formed by overlapping dissolution sites in the interlaminar region. If an idealized interlaminar region is considered, uniformly 25 μm thick, then the minimum ILT particle areal density required for such film formation can be easily estimated. Consider *Figure 7a*. For a thermoplastic particle to dissolve so as to completely fill the local interlaminar volume requires:

$$V=25\times10^{-4}\pi\frac{d^2}{4} \quad (1)$$

where V can be approximated by the original ILT particle volume, and d is the diameter of the dissolution site in cm. Assuming that the ILT particles were initially spherical, and that all had a diameter of 80 μm, gives:

$$V=\frac{4}{3}\pi\,(40\times10^{-4})^3 \quad (2)$$

in cm^3.

Substituting this value of V into equation (1), gives $d^2=1.36\times10^{-4}$ cm^2. The minimum ILT particle areal density on the prepreg to just form a 'film' of dissolution sites is then d^{-2} (see *Figure 7b*) (i.e. $\sim7.3\times10^3$ particles cm^{-2}). Hence at ILT particle areal densities higher than this, such film formation can be expected. This corresponds well with the laminate G_{1c} data in *Figures 5* and *6*, and film formation at $>6\times10^3$ particles cm^{-2} was confirmed by scanning electron

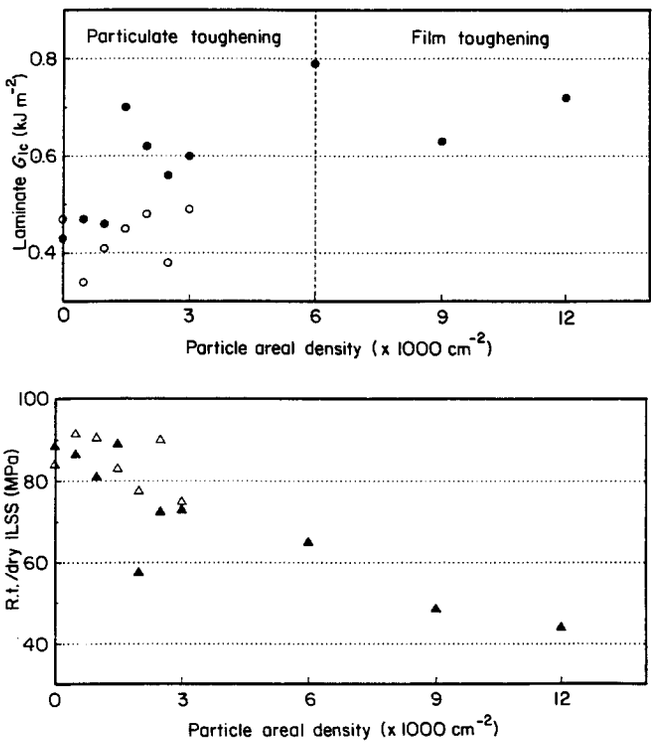

Figure 6 Laminate G_{1c} and ILSS for Hy-E 1686N, with thermoplastic A (●, ▲) or thermoplastic B (○, △) as the ILT agent

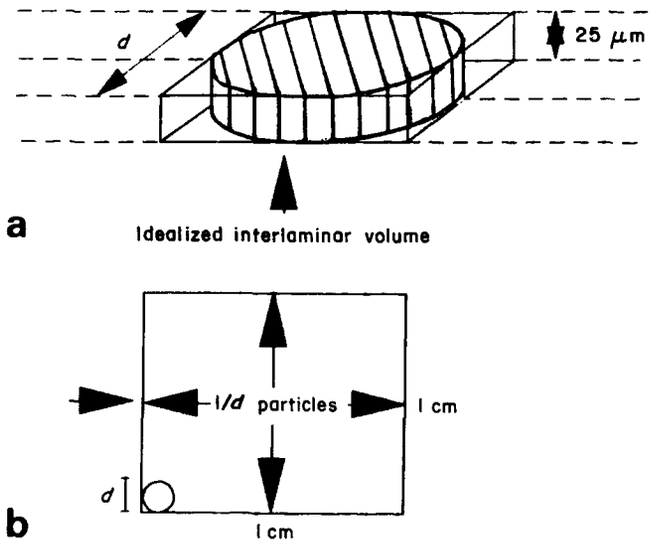

Figure 7 Dissolution of a thermoplastic particle in an idealized composite interlaminar region: (a) filling the interlaminar volume; (b) plan view showing the minimum areal density of dissolved particles for film formation.

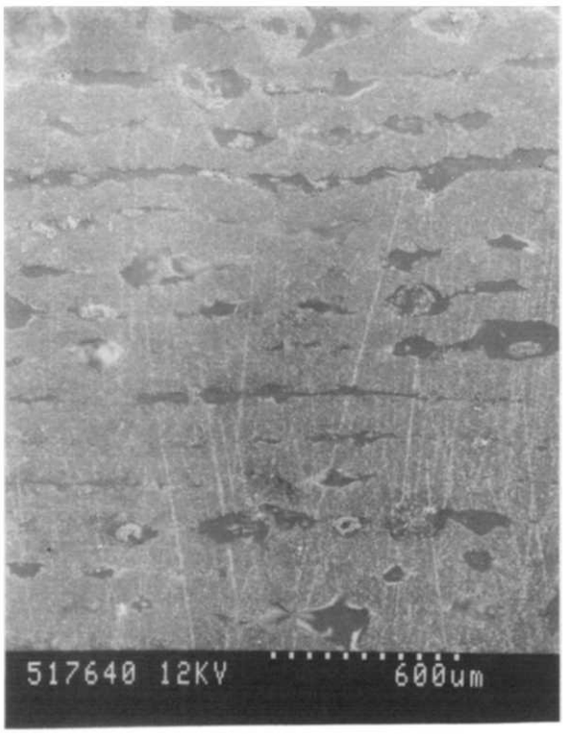

Figure 8 Film formation in Hy-E 1374BM with thermoplastic A as the ILT agent due to overlapping dissolution sites. ILT particle areal density on the prepreg $\sim 12 \times 10^3$ particles cm^{-2}

microscopy (*Figure 8*). This calculation is obviously not exact, as the tendency of the ILT particles to locally force the interlaminar region wider than 25 μm, and the dilution effect of blending with the thermoset have both been ignored. No definite boundary between particulate and film toughening at 7.3×10^3 particles cm^{-2} should therefore be inferred. It is nonetheless informative to see the above calculated value fall at least within the range expected from experimental results. Thus a secondary toughening mechanism exists here, when the final particle diameter is similar in magnitude to the original inter-particle spacing on the prepreg. It can thus be appreciated that the thermoplastic loading of the interlaminar region, in this case, is very much higher than that for the low ILT particle areal densities.

A calculation like the above for combination 3 is pointless, however, due to the fact that there was no significant improvement in laminate G_{1c} for $0\text{–}3 \times 10^3$ particles cm^{-2} of thermoplastic B added. Indeed for ILT particle areal densities higher than this, the test samples delaminated during the post-cure stage of their fabrication. Such a marked change can only be attributed to the difference in end group functionality with thermoplastic B, (which was otherwise identical to thermoplastic A). The non-reactive end groups of thermoplastic B have thus had a highly detrimental effect on toughness, if not on phase separation. This behaviour is also common in blended thermoplastic toughened thermosets; such a result was therefore to be expected[9,10].

The ILSS data for combinations 2 and 3 showed a slow fall with increasing ILT particle areal density on the prepreg (see *Figures 5* and *6*). The gradient for the room temperature/dry data decreased by ~ 4 MPa per 1×10^3 particles cm^{-2} added. It may, however, be possible to optimize the toughening in the low ILT particle areal density region for combination 2, whilst maintaining ILSS. Note that combination 1 showed no such fall in ILSS from $0\text{–}12 \times 10^3$ particles cm^{-2} added, for either the room temperature/dry or the hot/wet testing conditions. The ILSS performance may thus be related to the morphology adopted at the dissolution sites. Phase inversion (with a localized thermoplastic-rich continuum), apparently degrades ILSS more than a particulate morphology (with a localized thermoset-rich continuum).

Combinations 4–7

Figure 9 shows the morphology of a dissolution site for a thermoplastic C particle in combination 5. The results of the scanning electron microscopy of combinations 4 and 6 were very similar, namely that there was

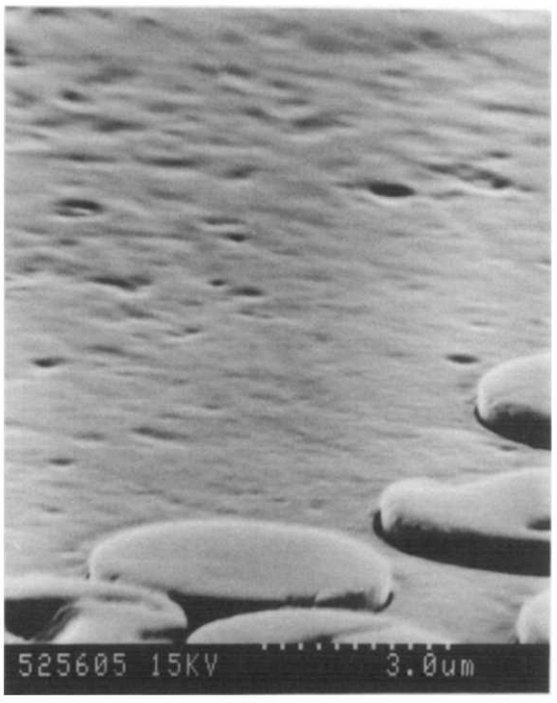

Figure 9 Two-phase morphology at the dissolution site of a thermoplastic C particle in Hy-E 1377-2T

evidence of a two-phase morphology. The exact nature of this morphology was difficult to determine, however, due to its much smaller scale than previous examples. (*Figure 9* is a micrograph of a polished and etched cross-section as before, but the angle of incidence is now 85° and not 0°). The morphology at dissolution sites in combination 7 was particulate in nature (i.e. comparable to *Figure 2*).

From the calculation above, at the low ILT particle areal densities of thermoplastic C used here (maximum $\sim 4.9 \times 10^3$ particles cm^{-2}), it is unlikely that film formation has occurred. This should be borne in mind when considering the CAI results of *Table 2*. The average percentage improvement over the control values for combinations 4–7 was 15%, which is significant given the small amount of thermoplastic C required. Undoubtedly the most graphic demonstration of the benefits of this ILT technique, however, was the reduction in the delamination area due to 6.67×10^3 J m^{-1} impact. A typical example of this is shown in *Figure 10* for combination 7. Delamination was effectively reduced in each of the four test laminates, at the $\sim 1.1 \times 10^3$ particles cm^{-2} loading, from $18.8 \pm 2.0\%$ to $7.7 \pm 1.0\%$ of the laminate area. For the 15 cm × 10 cm samples used, therefore, the average delamination area was reduced from 28.2 ± 3.0 cm^2 to 11.6 ± 1.5 cm^2 (down 59%). Compression resistance increased accordingly from 223.4 ± 0.7 MPa to 268.9 ± 15.9 MPa (up 20%) in this case.

Table 2 CAI data for ILT combinations 4–7

Combination	ILT particles cm^{-2} (× 1000)	CAI (MPa)	ILT CAI increase (%)
4	0	327.5 ± 6.9	–
4	3.4	364.7 ± 13.1	11 ± 6
5	0	258.6 ± 6.9	–
5	2.6	284.1 ± 12.4	10 ± 8
5	4.9	287.5 ± 17.2	11 ± 10
6	0	200.0 ± 6.9	–
6	3.1	242.0 ± 13.8	21 ± 11
7	0	223.4 ± 0.7	–
7	1.0	246.2 ± 12.4	10 ± 6
7	1.1	268.9 ± 15.9	20 ± 7
7	1.2	264.1 ± 9.7	18 ± 5
7	2.0	266.8 ± 11.0	19 ± 6

CONCLUSIONS

Novel, reactively terminated, polysulphone thermoplastics have been used as particulate interlaminar toughening agents in epoxy, bismaleimide and cyanate ester resin

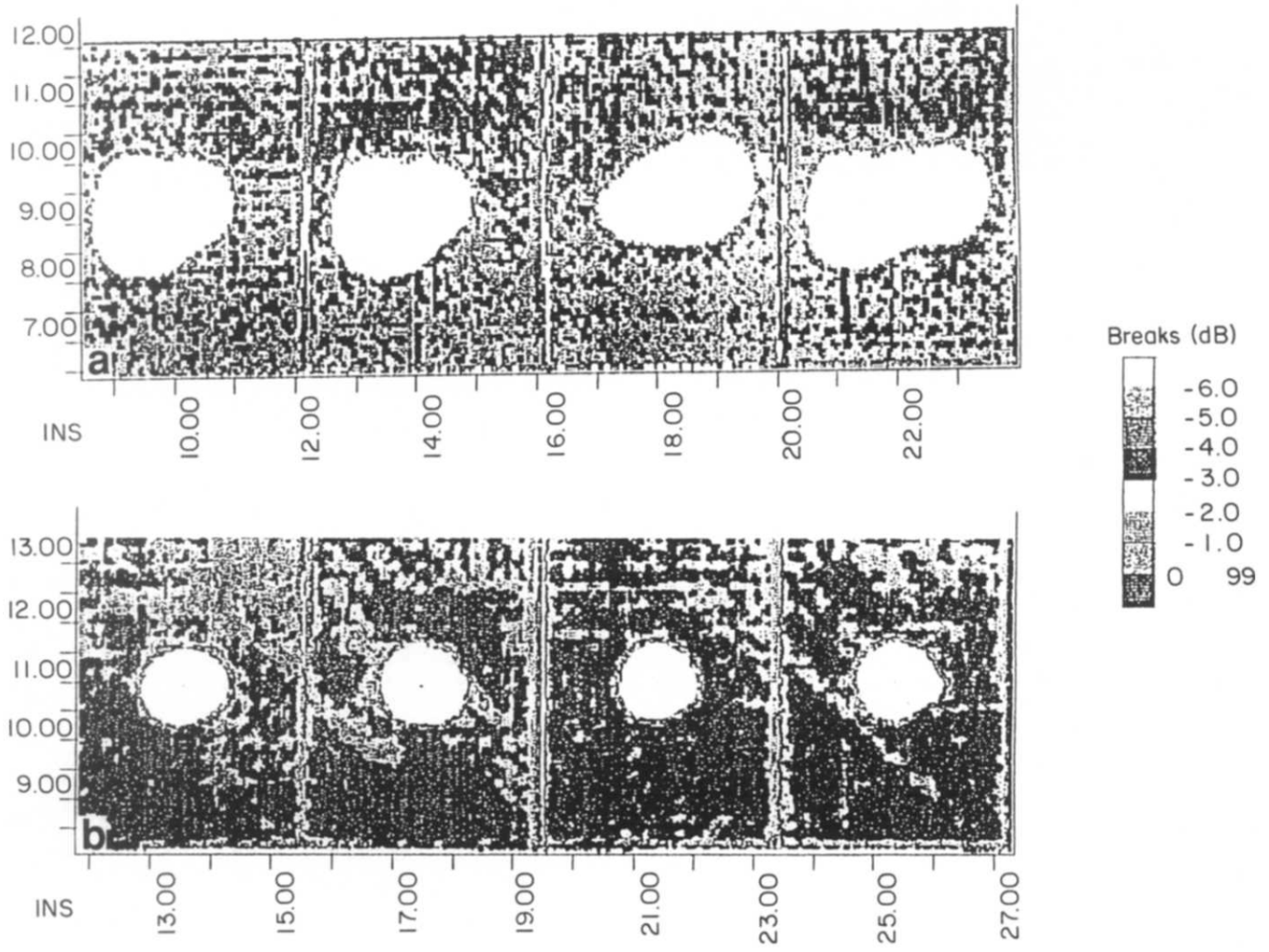

Figure 10 Ultrasonic C-scans of CAI test laminates after 6.67×10^3 J m^{-1} impact for (a) Hy-E 1354-2T and (b) Hy-E 1354-2T with thermoplastic C as the ILT agent. ILT particle areal density on the prepreg $\sim 1.1 \times 10^3$ particles cm^{-2}

based composites. These particles dissolved completely into the thermoset resin matrix during cure, resulting in two separate toughening effects. At low ILT particle areal densities on the prepreg, a maximum in laminate G_{1c} was measured by DCB testing. Here the thermoplastic-rich dissolution sites of these particles remained discrete. At higher ILT particle areal densities, however, these sites overlapped, and more continuous films of toughened thermoplastic-rich material were formed in the interlaminar regions. The improvements in laminate G_{1c} obtained (up to 84%), were shown to be strongly dependent on the end group functionality of the thermoplastic ILT agent used. There is a need for chemical reaction of this thermoplastic into the thermoset matrix via its end groups, in order that toughening may occur.

Interlaminar shear strength was adversely affected by the inclusion of ILT thermoplastic particles for the bismaleimide resin based composite. A fall of ~ 4 MPa per 1×10^3 particles cm^{-2} added was recorded for room temperature/dry testing. This effectively meant that only low ILT particle areal densities gave promising results in this case. No deterioration in ILSS was recorded with one epoxy resin based composite.

The CAI performance of various epoxy and cyanate ester resin based composites was also improved after such interlaminar toughening. The latter showed an increase from the control of 223.4 ± 0.7 MPa to 268.9 ± 15.9 MPa with only $\sim 1.1 \times 10^3$ particles cm^{-2} added. The impact was at 6.67×10^3 J m^{-1}. The delamination area was correspondingly reduced from 28.2 ± 3.0 cm^2 to 11.6 ± 1.5 cm^2.

ACKNOWLEDGEMENTS

The authors thank their colleagues at Wilton Materials Research Centre for their help with this work, and P. D. Mackenzie and V. Malhotra at ICI Fiberite for providing the CAI data.

REFERENCES

1 Hercules, US patent 4 863 787, 1989
2 Toray, European patent 0 274 899, 1987
3 Amoco, European patent 0 351 028, 1989
4 BASF, US patent 4 778 716, 1988
5 American Cyanamid, US patent 4 604 319, 1984
6 American Cyanamid, US patent 4 539 253, 1985
7 Boeing Material Specification 8-276, Boeing Corporation
8 Kinloch, A. J. and Young, R. J. 'Fracture Behaviour of Polymers', Elsevier, London, 1988, p. 434
9 Sefton, M. S., McGrail, P. T., Peacock, J. A., Wilkinson, S. P., Crick, R. A., Davies, M. and Almen, G. Proc. 19th Int. SAMPE Tech. Conf., 1987, p. 700
10 Almen, G. R., Mackenzie, P., Malhotra, V., Maskell, R. K., McGrail, P. T. and Sefton, M. S. Proc. 20th Int. SAMPE Tech. Conf., 1988, p. 46
11 Yamanaka, K. and Inoue, T. *Polymer* 1989, **30**, 662
12 Lange, F. F. and Radford, K. C. *J. Mater. Sci.* 1971, **6**, 1197